

Supporting Information

Unexpected phosphodiesterase activity at low pH of a dinuclear copper- β -cyclodextrin complex

Meng Zhao, Han-Lu Wang, Li Zhang, Cunyuan Zhao, Liang-Nian Ji and Zong-Wan Mao*

*MOE Key Laboratory of Bioinorganic and Synthetic Chemistry, School of Chemistry and Chemical
Engineering, Sun Yat-Sen University, Guangzhou 510275, China*

E-mail: cesmzw@mail.sysu.edu.cn

Abbreviations

H-BPMP = 2,6-bis[(bis(2-pyridylmethyl)amino)methyl]-4-methylphenol, PBTPA =
N,N'-((6,6'-(1,4-phenylene)bis(pyridine-6,2-diyl))bis(methylene))bis(1-(pyridin-2-yl)-N-(pyridin-2-ylmethyl)methanamine); PyBCD = 2,6-bis(6-mono-amino- β -cyclodextrin-methyl)-pyridine.

Experimental Procedures

Materials: Bis(4-nitrophenyl) phosphate (BNPP) and Diethyl phosphate (DEP) were purchased from Aldrich Chemical Company, and used without further purification. Di(*p-tert*-butylbenzyl) amine (DBBA) were synthesized by literature procedures (see 5d in article references). β -CD of reagent grade was recrystallized twice from H₂O and dried in vacuum for 12 h at 373 K. DMF were dried over CaH₂ for 2 days and then distilled under reduced pressure prior to use. Water used in all physical measurement experiments was Milli-Q grade.

Physical Measurements: Elemental contents were analyzed by a Perkin-Elmer 240 elemental analyzer. IR spectra were recorded on a Bruker FTIR EQUINOX 55 spectrometer. ESI-MS spectra were performed on a Thermo LCQ-DECA-XP spectrometer. UV-vis spectra were monitored with a

Varian Cary 300 UV/Vis spectrophotometer equipped with a temperature controller (± 0.1 K). Variable-temperature magnetic susceptibility data were measured using a Quantum Design MPMS7 SQUID magnetometer in the temperature range 2-300 K with an applied field of 10.0 kG.

Potentiometric Titration: An automatic titrator (Metrohm 702GPD Titrino) coupled to a Metrohm electrode was used and calibrated according to the Gran method.¹ The electrode system was calibrated with buffers and checked by titration of HClO₄ with NaOH solution (0.10 M). The thermostated cell contained 25 mL of 1.0 mM species in aqueous solutions with the ionic strength maintained at 0.10 M by sodium perchlorate. All titrations were carried out on the aqueous solutions under nitrogen at 298 ± 0.1 K, and initiated by adding fixed volumes of 0.10 M standard NaOH in small increments to the titrated solution. Triplicate measurements were performed, for which the experimental error was below 1 %. The titration data were fitted from the raw data with the Hyperquad 2000 program to calculate the $\log\beta$ and the pK_a values of species.

Theoretical calculations: The theoretical calculations were carried out on the model complex by optimizing the structure at the HF level with the Gaussian 03 program.² The basis sets used were LANL2DZ basis and pseudo potentials for Cu, and 3-21G for the rest of the atoms.

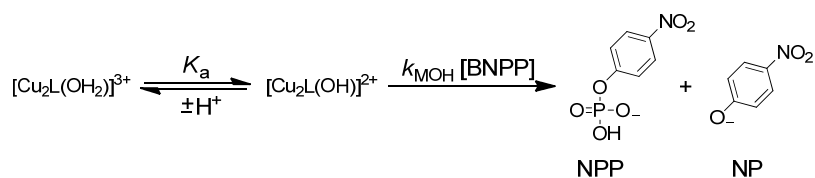
Kinetic Experimental Details: The rate of BNPP cleavage was measured by an initial slope method following the increase in the 400 nm absorption of the released 4-nitrophenolate (NP) in aqueous solution at 308 ± 0.1 K. At this wavelength, the absorbance of the ester substrate was negligible. Acetate (pH 4.20-5.20), MES (pH 5.70-6.80), MOPSO (pH 6.80-7.20), HEPES (pH 7.20-8.10), TAPS (pH 8.10-9.00), and CHES (pH 9.00-9.60) buffers were used (50 mM), and the ionic strength was adjusted to 0.1 with NaClO₄. The pH of the solution was measured after each run, and all kinetic runs with pH variation larger than 0.1 were excluded. The substrate BNPP, buffers, and complex in aqueous solution were prepared freshly. The reactions were initiated by injecting a small amount of BNPP into the buffer solutions of Cu₂L and followed by fully mixing at 308 ± 0.1 K. The visible absorption increase was recorded immediately and was followed generally until 2% formation of 4-nitrophenolate, where ϵ values for 4-nitrophenolate were 183 (pH 4.29), 278 (pH 4.73), 566 (pH 5.19), 1 355 (pH 5.71), 2 922 (pH 6.10), 4 201 (pH 6.48), 7 428 (pH 6.87), 9 700 (pH 7.12), 11 589 (pH 7.35), 12 844 (pH 7.51), 13 525 (pH 7.62), 14 340 (pH 7.74), 15 376 (pH 7.95), 15 527 (pH 8.10), 17 120 (pH 8.48), 17

400 (pH 8.61), 17 730 (pH 8.82), 17 970 (pH 9.02), 18 205 (pH 9.33), 18 320 (pH 9.55), and 18 370 (pH 9.80) at 400 nm. For the small extinction coefficient of NP in acidic solution, in some low pH runs the concentrations of Cu_2L and BNPP are both enlarged properly.

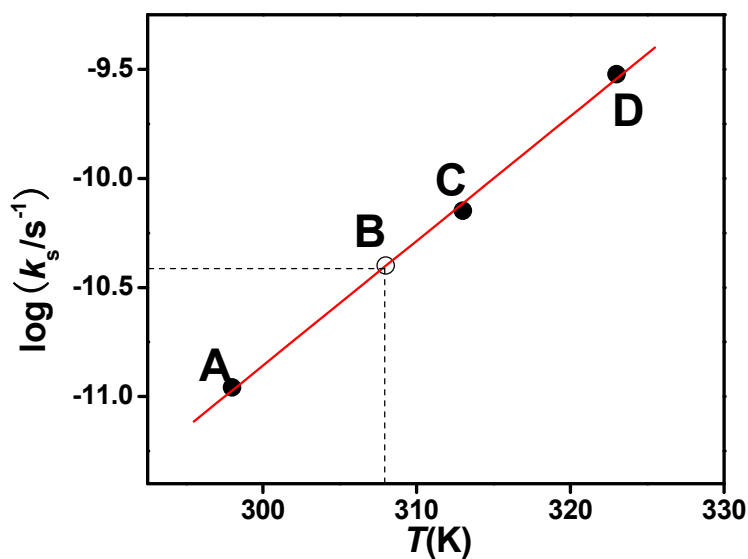
The pseudo-first-order rate constants of Cu_2L , k_{obs} (s^{-1}), were obtained directly from a plot of the 4-nitrophenolate concentration versus time by the method of initial rates which was linear with $R > 0.995$. To correct for the spontaneous cleavage of BNPP, each reaction was measured against a reference cell which was identical to the sample cell in composition except for the absence of Cu_2L . Errors on k_{obs} values were about 5%. The pseudo-first-order rate constants k_{obs} (s^{-1}) at different Cu_2L concentrations were measured. Then, the second-order rate constants k ($\text{M}^{-1}\text{s}^{-1}$) were determined as the slope of the linear plots of k_{obs} versus Cu_2L concentration. The second-order rate constants k ($\text{M}^{-1}\text{s}^{-1}$) at different pH were measured respectively and collected in pH-rate profiles (see Fig. 3 in article, Solid circle). The data was fit into the logarithmic form of eqn 1 which was derived from Scheme S1.

$$k = \frac{k_{\text{MOH}}K_{\text{a}}}{[\text{H}^+] + K_{\text{a}}} \quad \text{eqn 1}$$

Scheme S1.



The effect of BNPP concentration (shown as Fig. 4 in main article) was carried out by varying the BNPP concentration at constant concentration of the catalyst Cu_2L . The non-catalyzed reaction constant $k_{\text{uncat}} = 4.0 \times 10^{-11} \text{ s}^{-1}$ for BNPP spontaneous hydrolysis in water at 308 K is determined from the corresponding correlation between rate constants and temperature which is obtained from reported data (see the figure below): A and D is from ref. 16 (in main Article references), C is from ref. 3 (in ESI[†] references), B is the data we determined by extrapolation.



The inhibition study was carried out by varying the inhibitor concentration at constant concentrations of **Cu₂L** and BNPP. The inhibition data is fit to equation 2.

$$\frac{k_{\text{obs}}}{k_o} = \frac{K_i}{(K_i + [\text{Inhibitor}])} \quad \text{eqn 2}$$

Synthesis of **Cu₂L**

The ligand was synthesized as described in ref. 5c in article. To an aqueous solution (4 mL) of the ligand HL (0.100 g, 0.036 mmol), Cu(ClO₄)₂·6H₂O (0.032 g, 0.086 mmol) was added with magnetic stirring at room temperature for 0.5 h. Then, the solution was concentrated under vacuum, and poured into acetone (30 mL). The light green precipitate was collected by filtration, and washed with a small amount of ethanol. After dried in vacuum, the pure light green compound **Cu₂L** (0.099 g, 83%) was obtained (Found: C 39.46, H 5.96, N 1.75. C₁₀₅H₁₅₉N₄O₆₉·Cu₂(μ-OH)(ClO₄)₂·15H₂O requires C 39.48, H 5.99, N 1.75%); IR (KBr): ν = 3408, 2926, 1636, 1445, 1154, 1083, 1032, 943, 856, 757, 706, 677, 629, 579, 488 cm⁻¹; λ_{max}(H₂O)/nm 256 (ε/M⁻¹ cm⁻¹ 9180), 287 (4468), 340 (1051), 410 (448), and 628 (174); m/z (ESI-MS) 1353.5 (M + 2Cu²⁺ - 2H⁺, 100%).

Characterization Analysis

Fig. S1 shows the ESI-MS spectrum of **Cu₂L** which is detected in neutral aqua. The dominant spectra of $m/z = 1353.5$ corresponds to $[\text{Cu}_2\text{LH}_1]^{2+}$ strongly supports for a dinuclear Cu(II) complex. Since coordinated water or hydroxyl could not be detected under the ESI-MS condition, the two lost protons are both from the ligand. However, when the **Cu₂L** solution of is acidified to pH 2.3, a dominant mono-Cu(II) species is observed as shown in **Fig. S2**. These results are consistent with the species distribution curves (see **Fig. 2** in Main Article).

Elemental analysis results indicate a hydroxyl anion ligand is required for charge balance. The exogenous ligand is assigned to be a bridging μ -hydroxo one as suggested by the band at 677 cm^{-1} in the IR spectra⁴ (**Fig. S3**). The magnetic susceptibility data (**Fig. S4**) are fitted according to ref 5b in Main Article for exchange-coupled pairs of Cu(II) ions. The following parameters were obtained: $g = 2.06$, $2J = -106.9\text{ cm}^{-1}$ ($R^2 = 0.99858$), which are close to the reported dinuclear (μ -phenoxo)(μ -hydroxo) Cu(II) complex (ref 12a in Main Article). The above results confirm Cu(II) ions are doubly bridged in **Cu₂L**.

Fig. S4 shows UV-visible spectra of **Cu₂L** in solution. The pH was gradually adjusted from 2.2 to 12.7 by sodium hydroxide. The blue shift around 290 nm suggests the coordination conversion from mono to dinuclear phenoxo-bridged Cu(II) complex.⁵ Moreover, the shoulder appeared around 340 nm at pH 7.0 signify doubly bridged (μ -phenoxo)(μ -hydroxo) Cu(II) core,⁶ which is in line with the above characterization and potential titration results. The single Cu(II) d-d transitions band observed at 663 nm shifted to 622 nm as pH was adjusted from acidic to neutral, due to a coordination change from a mono- to a dinuclear complex.

In addition, the potential titration shows that a terminal-bound water ligand ($\text{p}K_a = 10.4$) is present indicating each Cu(II) is pentacoordinate, in line with the fact that most Cu(II) ions in this kind of dinucleating compartmental ligands are pentacoordinate.⁷ The theoretical calculation is operated based on the above characterizations.

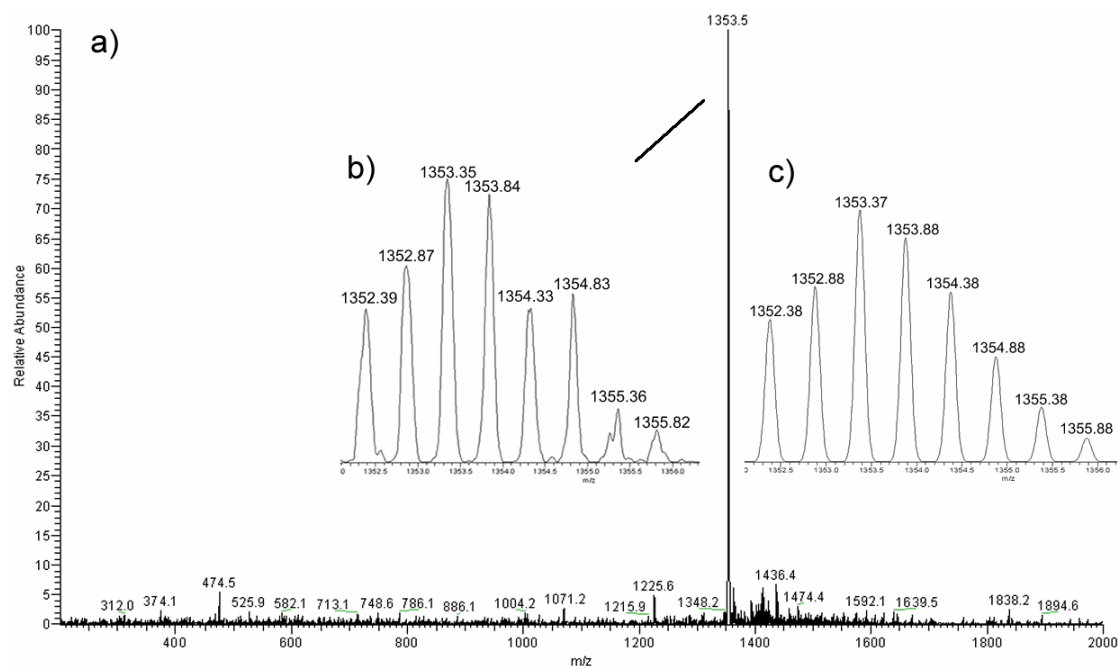


Fig. S1 Positive charge ESI-MS spectra of Cu_2L detected in a neutral solution: a) Full range spectra; b) Bivalence ion isotopes spectra detected; c) Bivalence ion isotopes spectra of computer simulation using formula $\text{C}_{105}\text{H}_{158}\text{N}_4\text{O}_{69}\text{Cu}_2$, corresponding to $[\text{Cu}_2\text{LH}_1]^{2+}$.

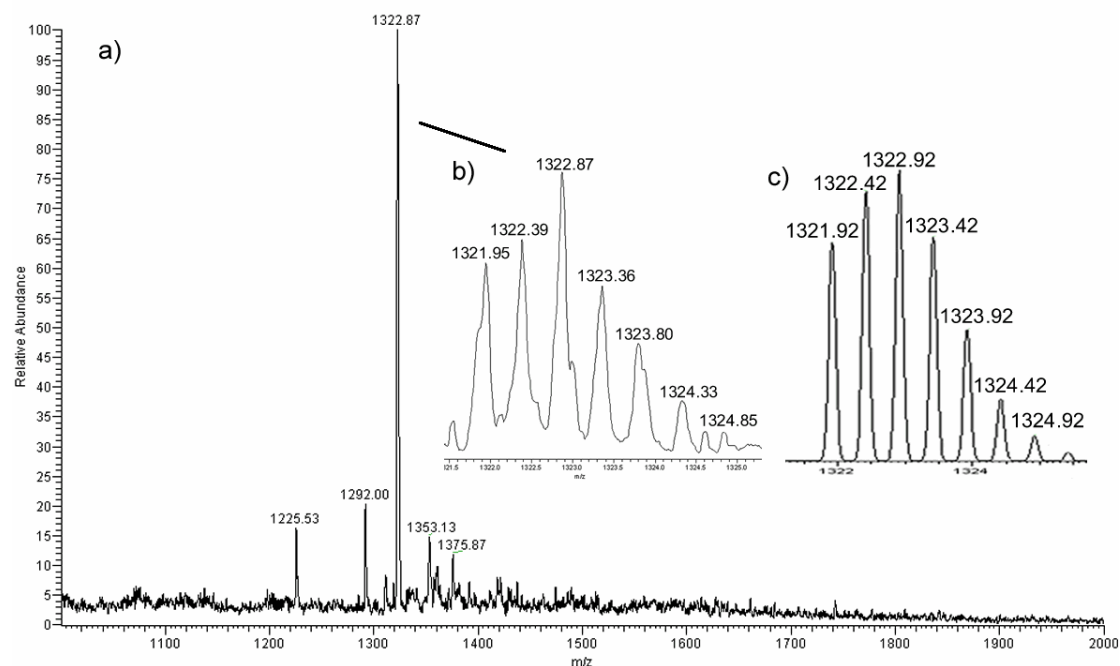


Fig. S2 Positive charge ESI-MS spectra of Cu_2L detected at pH 2.3: a) Full range spectra; b) Bivalence ion isotopes spectra detected; c) Bivalence ion isotopes spectra of computer simulation using formula $\text{C}_{105}\text{H}_{160}\text{N}_4\text{O}_{69}\text{Cu}$, which is equivalent with $[\text{CuLH}]^{2+}$.

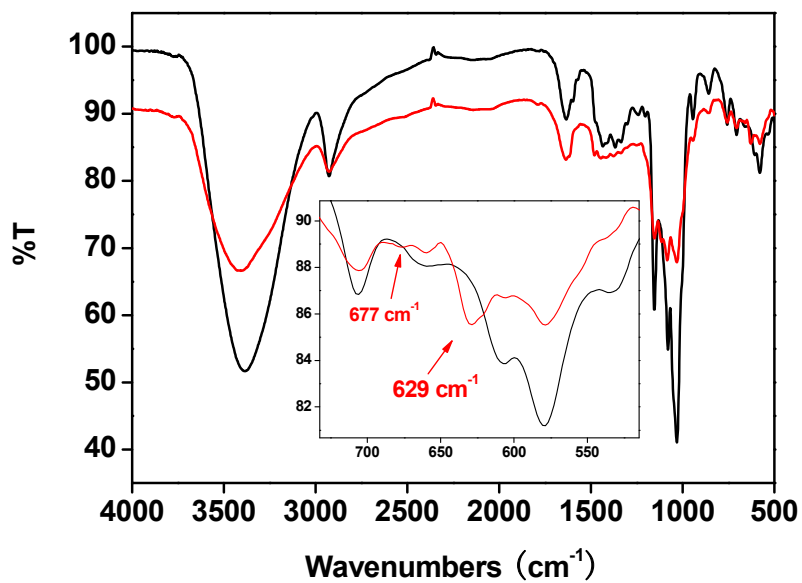


Fig. S3 IR spectra of ligand HL (in black) and complex Cu_2L (in red). The band at 629 cm^{-1} was assigned to the perchlorate anions.

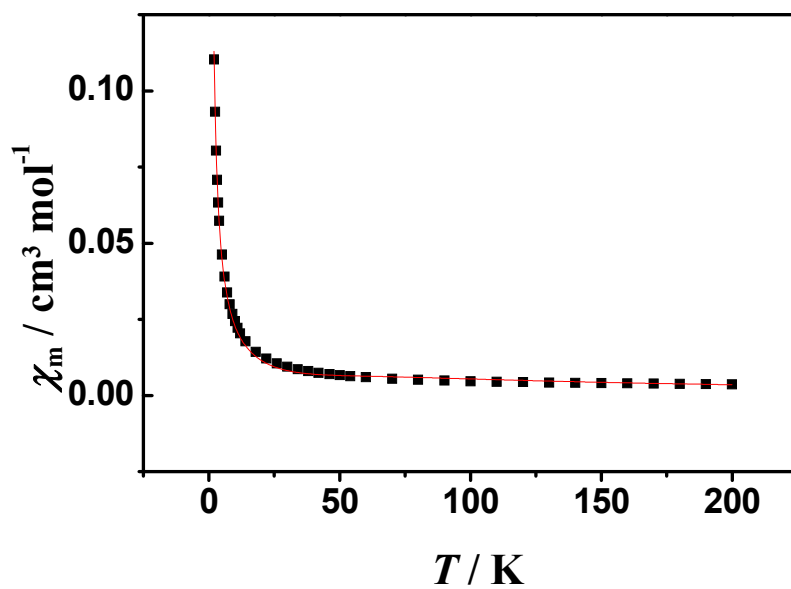


Fig. S4 Temperature dependence of the magnetic susceptibility for Cu_2L in the form χ_m vs T . The solid lines result from least-squares fit according to Bleaney-Bowers equation.

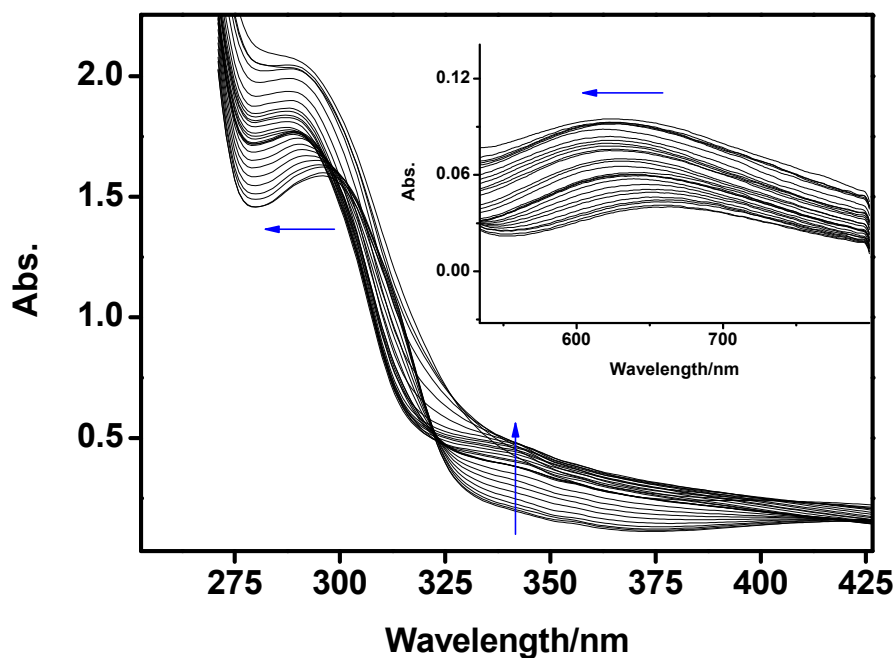


Fig. S5 UV-visible of Cu_2L (0.4 mM) at pH from 2.2 to 12.7 at 298 ± 0.1 K.

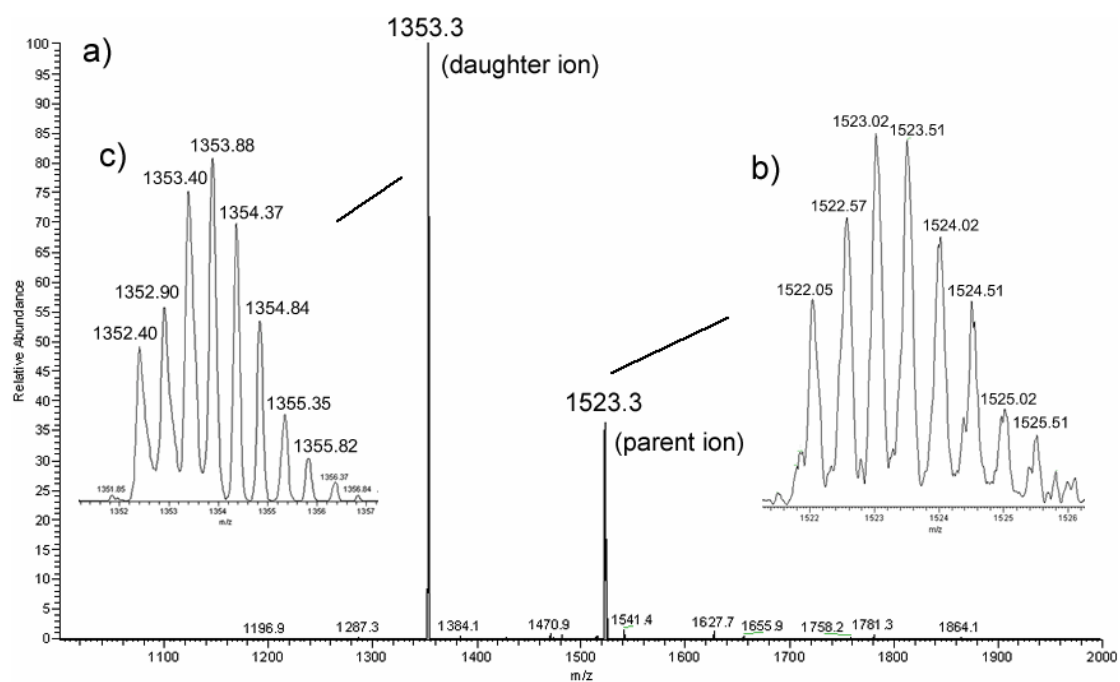


Fig. S6 a) Positive charge MS/MS spectra of the parent ion ($m/z = 1523.3$) detected in the sample of Cu_2L solution mixed with BNPP; b) Bivalence ion isotopes spectra of the parent ion; c) Bivalence ion isotopes spectra of the daughter ion. The result clearly indicates the parent ion corresponds to the species $[\text{Cu}_2\text{L}(\text{BNPP})]^{2+}$.

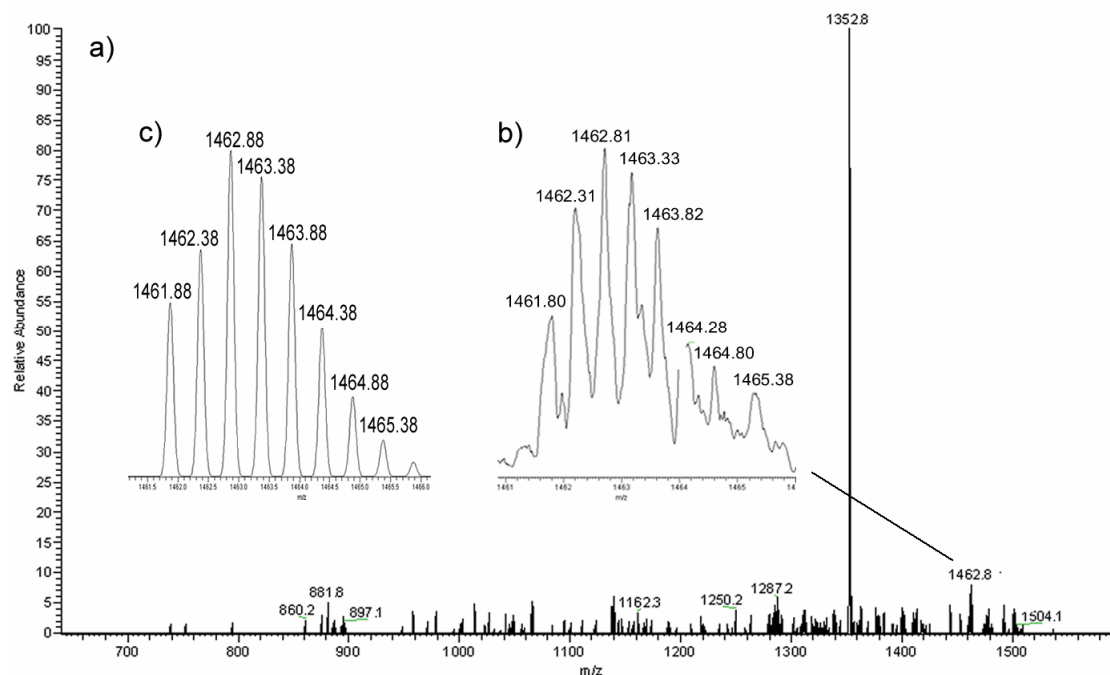


Fig. S7 a) Positive charge ESI-MS spectra of BNPP solution in the presence of Cu_2L which has been incubated overnight; b) Bivalence ion isotopes spectra detected; c) Bivalence ion isotopes spectra of computer simulation using formula $\text{C}_{111}\text{H}_{164}\text{N}_5\text{O}_{75}\text{PCu}_2$, which is equivalent with $[\text{Cu}_2\text{L}(\text{NPP})]^{2+}$ corresponding to a complex formed by $\text{Cu}_2\text{L}/\text{NPP}$ (1:1).

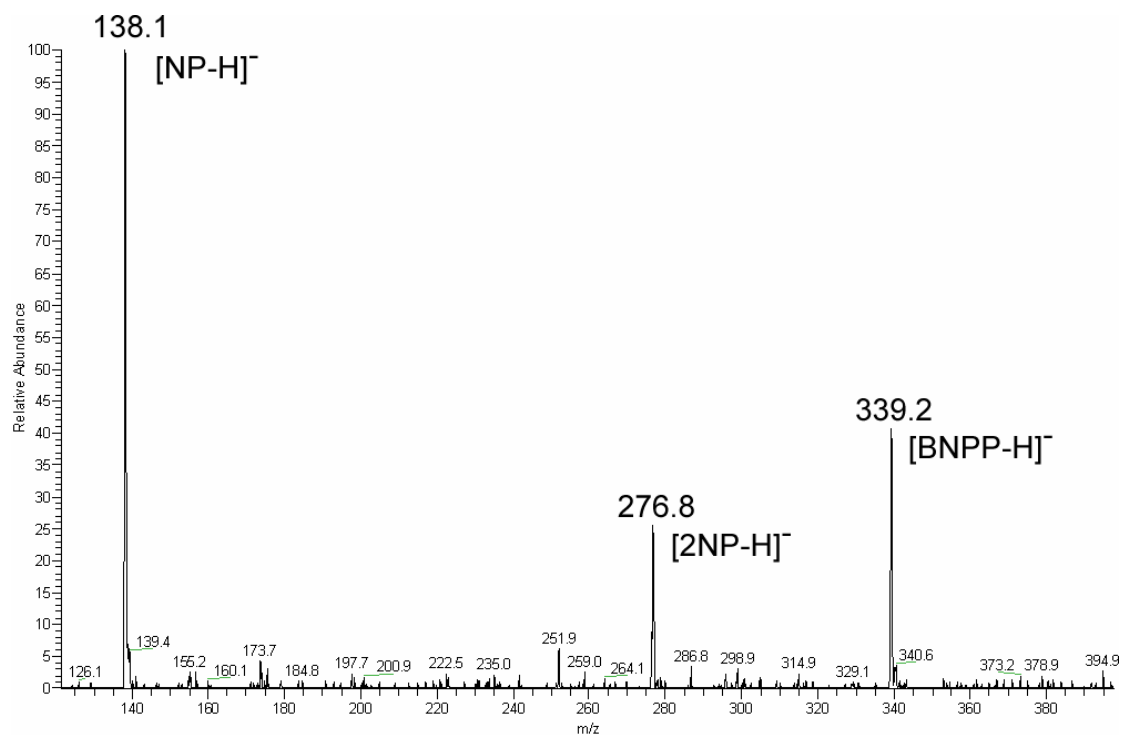


Fig. S8 Negative charge ESI-MS spectra of BNPP solution in the presence of Cu_2L .

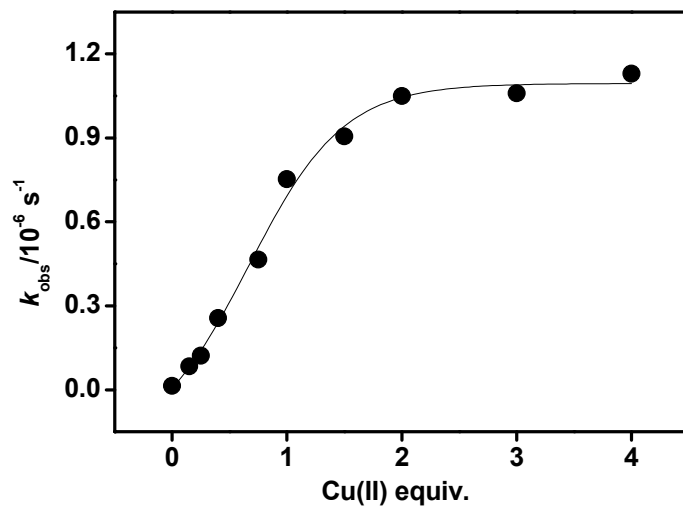


Fig. S9 Dependence of the rates of BNPP hydrolysis on the [Cu(II)]/[HL] ratio at constant HL and BNPP concentrations at pH 6.9, 308 ± 0.1 K, $I = 0.10$ M NaClO₄, and [buffer] = 50 mM. The solid line shows a Boltzmann fit of the data.

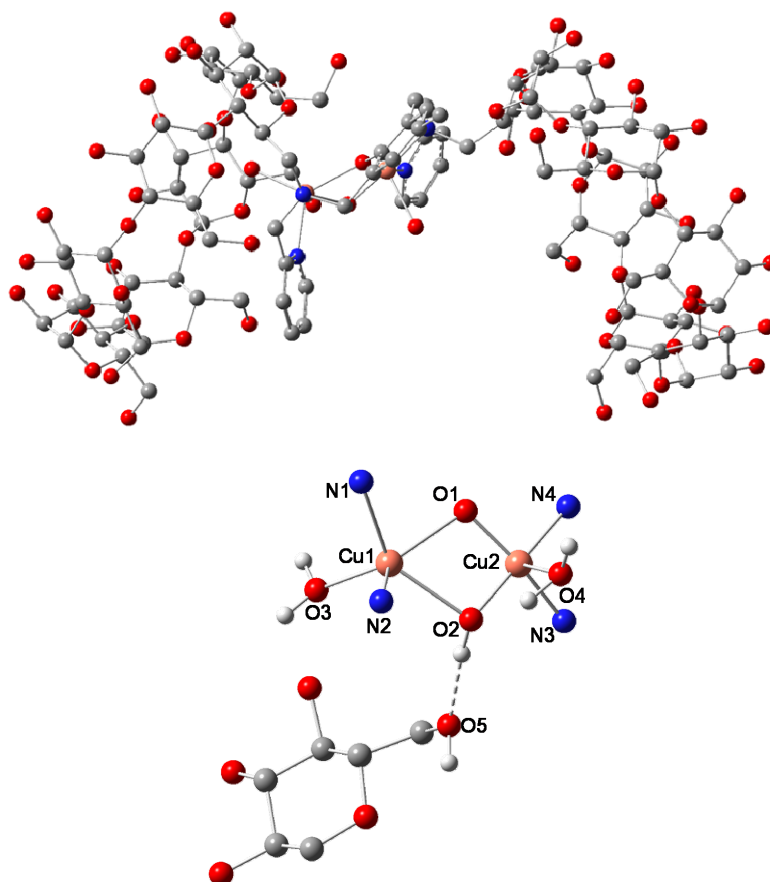


Fig. S10 (Top) top view of the calculated structure of Cu₂L omitting hydrogen atoms; (bottom) metal center, O5 represents the 6-hydroxyl residue on β -CD primary rim. Color code: grey, carbon; blue, nitrogen; red, oxygen; pink, copper.

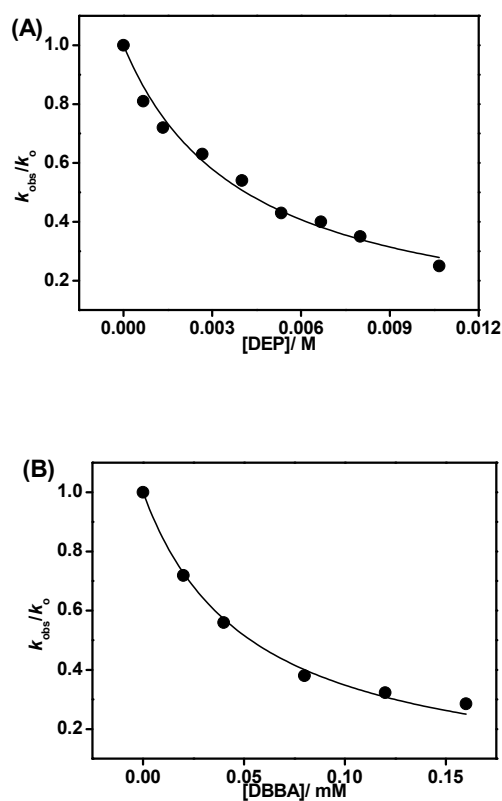
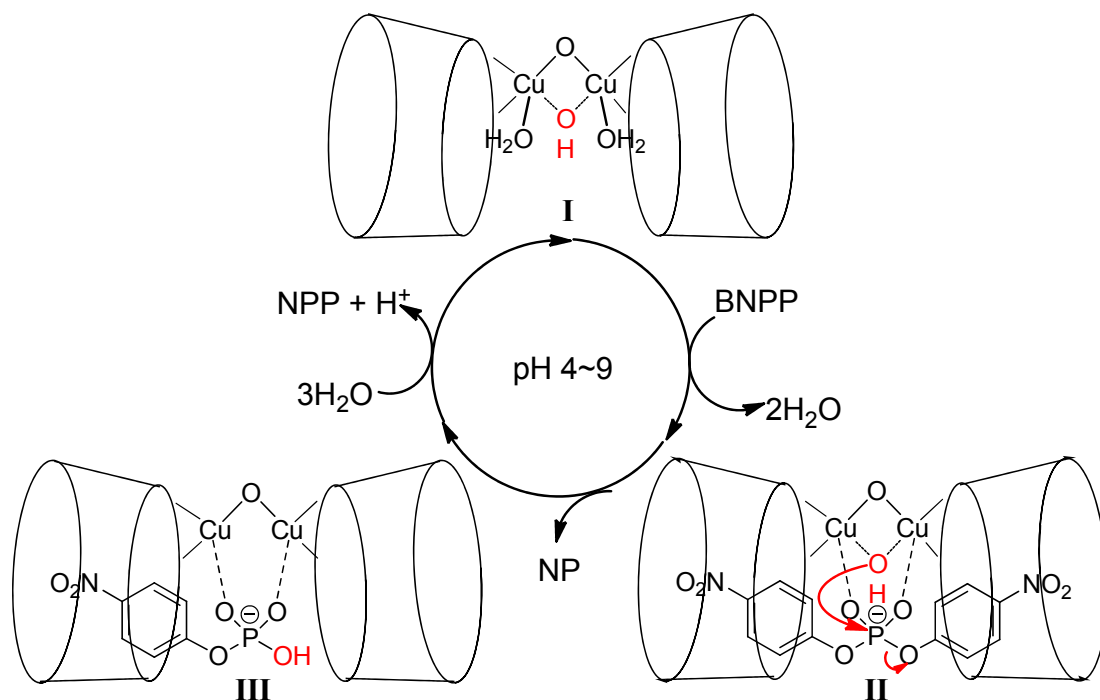


Fig. S11 Normalized pseudo-first-order rate constants for cleavage of BNPP at increasing concentration of (A) DEP and (B) DBBA, where k_0 is the observed first-order rate constant determined for reaction in the absence of inhibitor catalyzed by 0.1 mM Cu_2L in buffer (50 mM HEPES), $I = 0.1$ M (NaClO_4) at pH 7.2 and 308 ± 0.1 K. The solid line shows the fits of data to eqn 2 (ESI†) where the complex binds one molecule of inhibitor.

Table S1. Equilibrium constants of Cu_2L in aqueous solution at 298 ± 0.1 K.

| Species | Equilibrium constants | |
|---|-----------------------|---------------|
| | $\log\beta$ | $\text{p}K_a$ |
| $[\text{CuL}]^+$ | 23.3 ± 0.1 | — |
| $[\text{Cu}_2\text{L}]^{3+a}$ | 26.8 ± 0.1^b | — |
| $[\text{Cu}_2\text{L}(\text{OH})]^{2+}$ | 22.5 ± 0.1 | 4.3^c |
| $[\text{Cu}_2\text{L}(\text{OH})_2]^+$ | 12.1 ± 0.2 | 10.4 |

^a The species is assumed. ^b The data was calculated by extrapolation. ^c the data was determined from the non-linear fit of BNPP pH-rate profile according to eqn 1.



Scheme S2 The suggested mechanism of Cu_2L -catalyzed BNPP hydrolysis. The coordinate donor atoms are not shown for clarity, except for the bridging oxygen atoms. Complexes **I**, **II**, and **III** are all characterized by ESI-MS (Fig. S1, S6 and S7, ESI[†]).

References

- 1 G. Gran, *Acta. Chem. Scand.*, 1950, **4**, 559.
- 2 M. J. Frisch, G. W. Trucks, H. B. Schlegel, G. E. Scuseria, M. A. Robb, J. R. Cheeseman, J. A. Montgomery, Jr., T. Vreven, K. N. Kudin, J. C. Burant, J. M. Millam, S. S. Iyengar, J. Tomasi, V. Barone, B. Mennucci, M. Cossi, G. Scalmani, N. Rega, G. A. Petersson, H. Nakatsuji, M. Hada, M. Ehara, K. Toyota, R. Fukuda, J. Hasegawa, M. Ishida, T. Nakajima, Y. Honda, O. Kitao, H. Nakai, M. Klene, X. Li, J. E. Knox, H. P. Hratchian, J. B. Cross, V. Bakken, C. Adamo, J. Jaramillo, R. Gomperts, R. E. Stratmann, O. Yazyev, A. J. Austin, R. Cammi, C. Pomelli, J. W. Ochterski, P. Y. Ayala, K. Morokuma, G. A. Voth, P. Salvador, J. J. Dannenberg, V. G. Zakrzewski, S. Dapprich, A. D. Daniels, M. C. Strain, O. Farkas, D. K. Malick, A. D. Rabuck, K. Raghavachari, J. B. Foresman, J. V. Ortiz, Q. Cui, A. G. Baboul, S. Clifford, J. Cioslowski, B. B. Stefanov, G. Liu, A. Liashenko, P. Piskorz, I. Komaromi, R. L. Martin, D. J. Fox, T. Keith, M. A. Al-Laham, C. Y. Peng, A. Nanayakkara, M. Challacombe, P. M. W. Gill, B. Johnson, W. Chen, M. W. Wong, C. Gonzalez and J. A. Pople, *Gaussian 03, Revision D.01*, Gaussian, Inc., Wallingford CT, 2004.

- 3 N. V. Kaminskaia, C. He and S. J. Lippard, *Inorg. Chem.*, 2000, **39**, 3365.
- 4 J. R. Ferraro and W. R. Walker, *Inorg. Chem.*, 1965, **4**, 1382.
- 5 T. Gajda, A. Jancsó, S. Mikkola, H. Lönnberg and H. Sirges, *J. Chem. Soc., Dalton Trans.*, 2002, 1757.
- 6 (a) S. Torelli, C. Belle, I. Gautier-Luneau, J. L. Pierre, E. Saint-Aman, J. M. Latour, L. Le Pape and D. Luneau, *Inorg. Chem.*, 2000, **39**, 3526; (b) K. Selmeczi, M. Giorgi, G. Speier, E. Farkas and M. Réglér, *Eur. J. Inorg. Chem.*, 2006, 1022.
- 7 J. Reim and B. Krebs, *J. Chem. Soc., Dalton Trans.*, 1997, 3793.